NANO · MICRO small
www.small-journal.com

Atomically Precise Metal–Metal Oxide Interface in Polyoxometalate-Noble Metal Hybrid Clusters

Hai-Ning Wang, Xing Meng, Yitao Cao,* Shun-Li Li, and Ya-Qian Lan**

Metal-metal oxide hybrid materials, typically composed of metal nanoparticles anchored on metal oxides matrix, are devoted enormous attentions as famous heterogeneous catalysts. The interactions between noble metals and metal oxides as well as their interfaces have been proven to be the origin of their excellent catalytic performance. Deep understandings on the interactions between noble metals and metal oxides at atomic precision, thus to precisely assess their contributions to catalysis, can serve as basic principles for catalyst design. In recent years, polyoxometalates (POMs), which in principle can be regarded as atomically precise metal oxide clusters, have been shown to have strong affinity to noble metals, thus forming diverse kinds of POM-noble metal hybrid clusters. Their well-resolved atomically precise structures and hybrid nature promise them as ideal platforms to understand the interfaces and interactions between noble metals and metal oxides. In this review, metal-metal oxide interface is classified into different categories based on the different configurations of hybrid clusters, and aims to understand the interface structures and electronic correlations between POMs and noble metals at the atomic precision. Based on these basic understandings, the study provides the perspectives on the challenges and research efforts to be paid in the future.

1. Introduction

Metal-metal oxide hybrid materials have been extensively explored to be excellent heterogeneous catalysts in many important reactions with high activity and selectivity.[1] They are typically composed of isolated metal nanoparticles anchored on metal oxides matrix, in which the interfacial electron transfer and interface structures have been demonstrated to have significant impact on catalytic performance.[2] Tremendous research efforts have been paid to understand the interaction between metals and metal oxides, as well as their interfacial structures, thus to precisely assess their contributions and guide the rational design of metal-metal oxide hybrid materials. For example, Murray et al. found catalytic performances highly depend on the length of metal-ceria interfaces constructed from ceria and various size-tunable metal clusters.[3a] Moreover, the electron microscopy techniques were explored for observing interfacial structures of gold nanoparticles on metal oxide matrix successfully.[3b]

Despite of the achievements made, there still exists great challenges to be addressed.[4] Previous researches have revealed that the catalytic performances highly rely on the size of metal nanoparticles, types of metal oxide matrix, and especially the metal-metal oxide interface structure.[5] The metal-metal oxide interface composed of several layers of atoms needs precise understandings down to the atomic level. However, it is a difficult task to regulate the local structures of metal oxides, as well as the size and distribution of metal nanoparticles in metal-metal oxide hybrid materials. Currently, the accuracy of manipulation and characterization of metal-metal oxide hybrid materials have largely remained in nanoscale, forming a mismatch with the requirement of atomic-level understandings. There is an urgent need to fabricate model metal-metal oxide hybrid materials with atomic precision to precisely evaluate contributions of different structural parameters, and fundamentally understand the key factors determining catalytic performance.

Polyoxometalates (POM)-noble metal hybrid clusters provide opportunities to address this issue.[6] POMs, which in principle can be regarded as atomically precise metal oxide clusters,[7] prefer to incorporate various metals, for instance, noble metals (palladium, platinum, silver, and gold etc.), thus forming diverse kinds of POM-noble metal hybrid clusters. Until now, massive researches have been proposed, and as such we mainly focus on POM-noble metal hybrid clusters based on multi-noble metallic clusters with varied interface configurations. Crystalline POM-noble metal hybrid clusters own well-defined structures with the uniform composition, size, and shape, which can be characterized by single X-ray diffraction and mass spectrometric

H.-N. Wang, X. Meng
School of Chemistry and Chemical Engineering
Shandong University of Technology
Zibo 255049, P. R. China
E-mail: mengxing@sdut.edu.cn
Y. Cao, S.-L. Li, Y.-Q. Lan
School of Chemistry
National and Local Joint Engineering Research Center of MPTES in High Energy and Safety LIBs
Engineering Research Center of MTEES (Ministry of Education)
Key Lab. of ETESPG(GHEI)
South China Normal University
Guangzhou 510006, P. R. China
E-mail: cao_yitao@m.scnu.edu.cn; yqlan@m.scnu.edu.cn
The ORCID identification number(s) for the author(s) of this article can be found under https://doi.org/10.1002/smll.202408884

DOI: 10.1002/smll.202408884

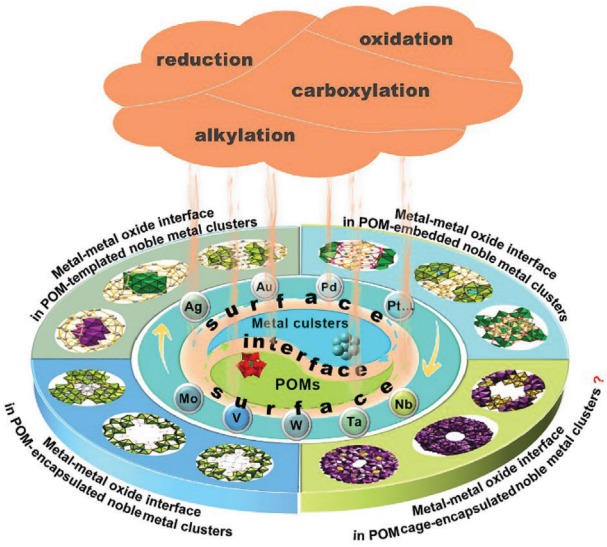

Scheme 1. The synthesis and potential applications of POM-noble metal hybrid clusters.

techniques at atomic precision. Their well-resolved atomically precise structures promise them as ideal platforms to understand the interfaces and interactions between metals and metal oxides. Currently, many achievements of POM-noble metal hybrid clusters have been made by several groups, such as Mak's group,[8] Sun's group,[9] and so on. With the help of these model platforms, understandings toward structure-property relationships at atomic level could be established, benefitting future research efforts to design novel catalysts.

Nowadays, several reviews have summarized and highlighted the structures and properties of POM-noble metal hybrid clusters, especially silver-containing hybrid clusters.[10] In this review, we focus on the interface chemistry between noble metals and metal oxides in POM-noble metal hybrid clusters, including metal-metal oxide coordination patterns as well as the electron transfer between them. Therefore, metal-metal oxide interface varies with the structure of POM-noble metal hybrid clusters, and can be classified into three categories according to the different configurations of hybrid clusters, including metal-metal oxide interface in POM-templated noble metal clusters, metal-metal oxide interface in POM-embedded noble metal clusters, and metal-metal oxide interface in POM-encapsulated noble metal clusters, which will give different interfaces between POMs and noble metals. Based on the classification, we aim to systematically understand the interface structures and electronic correlations at the atomic precision (**Scheme 1**). We hope this review can inspire more research works on this specific kind of hybrid clusters and guide the future research efforts on the atomic precise understandings of metal-metal oxide composites.

2. Metal-metal oxide interface in POM-noble metal hybrid clusters

Metal-metal oxide interface varies with the structure of POM-noble metal hybrid clusters. Based on the different configurations of hybrid clusters, metal-metal oxide interface in POM-noble metal hybrid clusters can be classified into three categories (**Figure 1**): 1) metal-metal oxide interface in POM-templated noble metal clusters, 2) metal-metal oxide interface in POM-embedded noble metal clusters, and 3) metal-metal oxide interface in POM-encapsulated noble metal clusters. The interface structures and electronic properties show prominent differences among different categories, naturally, our discussion will focus on the interface structure and interactions (charge transfer etc) between noble metals and POMs in different categories in the following sections.

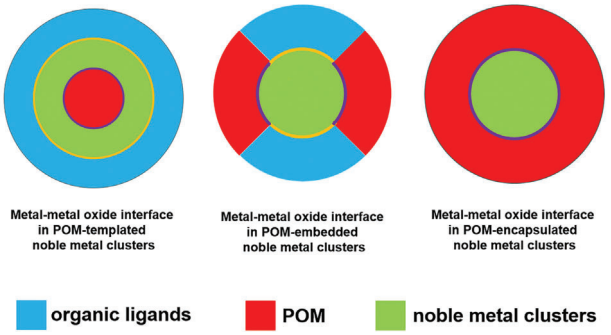

Figure 1. The POM-noble metal hybrid clusters with diverse interface configurations.

2.1. Metal-Metal Oxide Interface in POM-Templated Noble Metal Clusters

POMs can template the formation of POM-templated noble metal hybrid clusters by taking advantage of the anionic nature. Negatively charged POM anions can adsorb positively charged noble metal ions and induce the formation of core (POMs)-shell (noble metal) structures. Due to the high surface energy, the exposed noble metal surface needs to be further stabilized by organic ligands (alkynes etc). The coexistence of organic ligands and POMs contributes to the stabilization of a plentiful of hybrid clusters, whose structures are widely described in detail in the previous reports.[11] POMs guide the formation of the outside noble metal shell, which will significantly modify the physicochemical properties of hybrid clusters. In this section, we will pay attention to discussing the interface structure and interfacial electron transfer dominating the electrochemical and/or photoluminescent properties of representative examples.

Mak's group created $\{[Ag_{67}(PW_9O_{34})_2(p\text{-}F\text{-}PhS)_{36}(DMAc)_2(CF_3COO)_6]\bullet(CF_3COO)_7\cdot(DMAc)_x\}$ (Ag67) with lacunary Keggin $[PW_9O_{34}]^{9-}$ cores and Ag_{67} shells (**Figure 2a**),[12] where 12 Ag atoms in the middle of the cluster were coordinated with 12 terminal O atoms from $[PW_9O_{34}]^{9-}$ cores, with the length of Ag–O bonds from 2.236(2) to 2.594(2) Å. The remaining Ag atoms encircled two $[PW_9O_{34}]^{9-}$ cores through the coordination of Ag atoms with terminal O atoms as well as Ag···Ag interactions. Cyclic voltammograms (CV) were used to reveal the electrochemical property of Ag67 as well as other hybrid clusters (Figure 2b).[13] CV curves of hybrid clusters showed similar redox peaks to that of Ag(I) species in solution, indicating their redox behaviors were mainly derived from the outer silver(I) shell. However, CV curves still exhibited shifted peak positions,

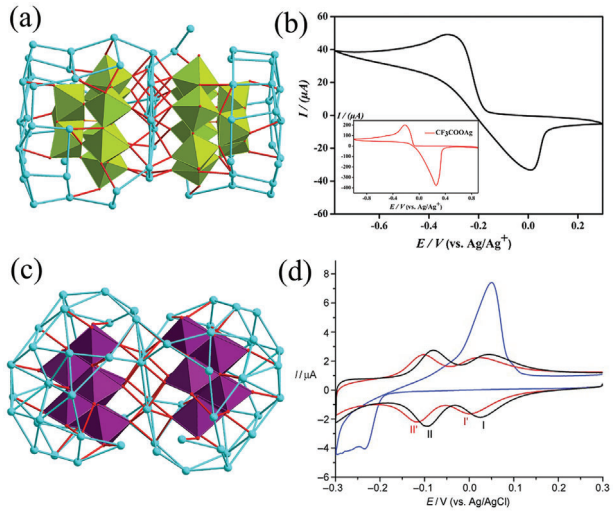

Figure 2. The structure of Ag67 showing the a) Ag–POM interactions, and b) its CV curve. c) The structure of Ag60 exhibiting the Ag–POM interactions, and d) CV plots of various electrodes resulting from GC/c-NF (black), GC/MO-NF (red), and GC/c (blue). (GC or NF = glassy carbon or Nafion, MO = $Mo_7O_{24}^{6-}$). Reprinted with permission.[12,13] Copyright 2018 American Chemical Society and 2010 Wiley-VCH respectively.

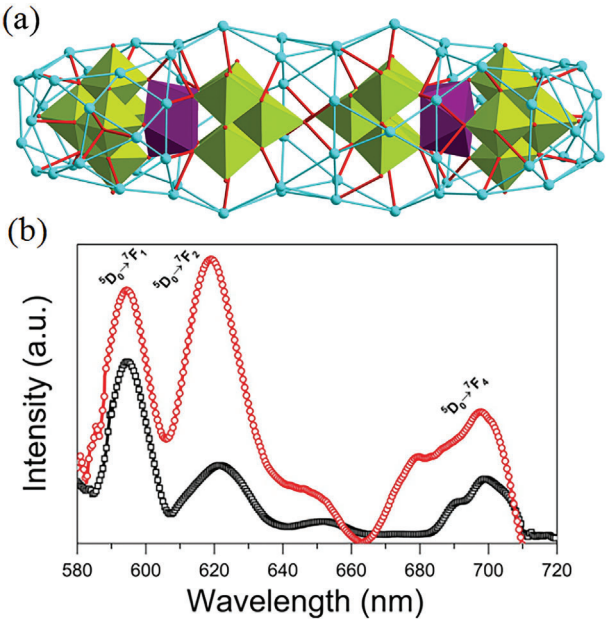

Figure 3. a) The structure of SD/Ag20 as well as Ag–POM interactions. b) The emission spectra of SD/Ag20 (red) and $Na_9[EuW_{10}O_{36}]$ (black). Reprinted with permission.[15b] Copyright 2018 Wiley-VCH.

indicating electron transfer between POM cores and noble metal shells could participate in the electrochemical process and play an impact on redox behaviors. The electron correlation between POM core and noble metal shell also influenced band gap structure of the hybrid cluster, which was dominated by filled $4d^{10}$ orbitals on Ag(I) of noble metal shells and empty $5d^0$ orbitals on W(VI) of POM cores.[12]

POM-templated noble metal clusters can also show different kinds of electrochemical properties as revealed in CV and/or differential pulse voltammetry results. Wang's group devoted great contributions in this field.[14] They employed various POM precursors (isopolyoxoanions, lacunary POMs, etc.) to obtain some giant POM-silver hybrid clusters. For example, $[Ag_{60}(Mo_6O_{22})_2(t\text{BuC}{\equiv}\text{C})_{38}](CF_3SO_3)_6$ (Ag60) was constructed from two $Mo_6O_{22}^{8-}$ ions as templates and an Ag_{60} shell (Figure 2c).[14d] Ag-O bonds bound $Mo_6O_{22}^{8-}$ cores and Ag_{60} shells together, and their lengths arranged from 2.039(6) to 2.573(5) Å. Their CV curves were recorded (Figure 2d), where the observed redox peaks possessed some differences compared to that of Ag(I) precursor. Alternatively, the analysis toward the peaks from CV curves revealed POM cores involved in the redox process. Silver shells did not take part in the redox process together with POMs but served as electron mediators transferring electrons between POM cores and the electrode, indicating the efficient core–shell electron correlation in the electrochemical process.

The interaction between POM cores and noble metal shells is also revealed in their optical properties, such as photoluminescence. Sun's group had discovered numerous POM-silver hybrid clusters and studied their photoluminescent properties.[15] The assembly between weakley-type $[EuW_{10}O_{36}]^{9-}$ and a silver cluster gave birth to $(EuW_{10}O_{36})_2@Ag_{72}(t\text{BuC}{\equiv}\text{C})_{48}Cl_2{\cdot}4BF_4$ (SD/Ag20) (**Figure 3a**),[15b] where two isolated $[EuW_{10}O_{36}]^{9-}$ were surrounded by Ag_{72} clusters via Ag-O bonds with distances from 2.487(18) to 2.86(2) Å. The emission spectrum of SD/Ag20 originating from Eu^{III} could be assigned to phosphorescence and exhibited similar characteristic peaks but enhanced intensities compared to those of $[EuW_{10}O_{36}]^{9-}$ (Figure 3b), suggesting that the outer silver cluster confined $[EuW_{10}O_{36}]^{9-}$ through Ag-O bonds effectively, hindering energy loss from molecular vibrations and influencing decay pathways of Eu^{III} emissions.

In this section, we discuss the analysis toward electrochemical properties of POM-templated noble metal clusters, which demonstrates that both POM cores and noble metal shells participate in the electrochemical process and synergistic effects between them. What's more, various POM-templated silver clusters usually exhibit fascinating photoluminescences, possibly ascribed to interactions between POM cores and noble metal shells, promising to be potential optical materials.

2.2. Metal-Metal Oxide Interface in POM-Embedded Noble Metal Clusters

Other than an anionic template, POMs can also act as multidentate ligands with vacant sites (lacunary POMs) in the construction of POM-embedded noble metal hybrid clusters. In this section, we will discuss the POM-embedded noble metal clusters in which the noble metal cluster is co-protected by POMs and/or organic ligands.[16] This kind of hybrid clusters are featured by a jointly occupation of their surface by organic and inorganic parts, showing more complicated interface strucutres. Our discussion will focus on their interface structures.

A hybrid surface constructed by bare POMs and organic ligands is presented in a sandwich-type hybrid nanocluster created by Jansen's group, exhibiting the formula $\{[Ag_{42}(CO_3)(C{\equiv}CtBu)_{27}(CH_3CN)_2][CoW_{12}O_{40}]_2\}^+$ (Ag42) based

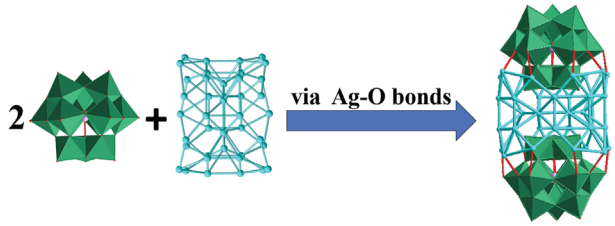

Figure 4. The self-assembly process of Ag42 with atomically precise interfaces.

on Ag_{42} clusters were embedded in two lacunary $[CoW_{12}O_{40}]^{6-}$ (**Figure 4**),[17] Ag_{42} clusters achieved a very rare and irregular circular shape, holding nine hexagons formed by six silver atoms via sharing the edge and six extra silver atoms linked together by the CO_3^{2-} anion locating at the center. $[CoW_{12}O_{40}]^{6-}$ occupied the upper and lower parts of Ag_{42} through Ag-O-W bonds, whose distances ranged from 2.517(1) to 2.778(9) Å between Ag and O atoms.

Except for POMs, titanium-oxo (Ti-oxo) clusters have also been extensively explored, and their bulky counterparts, titanium oxide (TiO_2) is one of the most important metal oxides to be used in metal-metal oxide composites. Considering our purpose to discuss the atomically precise metal-metal oxide interface, there are several hybrid clusters constructed by Ti-oxo clusters and noble metals which we cannot ignore in our discussion. Zhang and coworkers employed Ti-oxo clusters as protectants to stabilize Ag clusters and created several Ti-oxo-Ag hybrid clusters, which also provided accurate interfaces at the atomic scale.[18] In one of them, they described $[Ag_{14}Ti_{16}O_{24}(FBC)_{28}(tBuC{\equiv}C)_2]\cdot(H_2O)_4\cdot(Toluene)_3$ (Ag14@Ti16), where Ag_{14} rod clusters were implanted within $Ti_{16}O_{24}$ ring shells by means of Ag-O-Ti bonds (**Figure 5**).[18b] The structural analysis revealed that Ag_{14} rod clusters consisted of rhombus Ag_4 units sandwiched by two distorted pyramid Ag_5 units, and the outer $Ti_{16}O_{24}$ ring shells were assembled by overlapping two Ti_8 rings through 8 bridging oxygen atoms. To evaluate the electronic structures, several examples were investigated through Density functional theory (DFT) calculations.[19] The calculated results revealed that the highest occupied molecular orbital (HOMO) usually was situated in the deep core of Ag clusters, and the lowest unoccupied molecular orbital (LUMO) originated from Ti atoms and Ag clusters, indicating the direction of electron transitions.

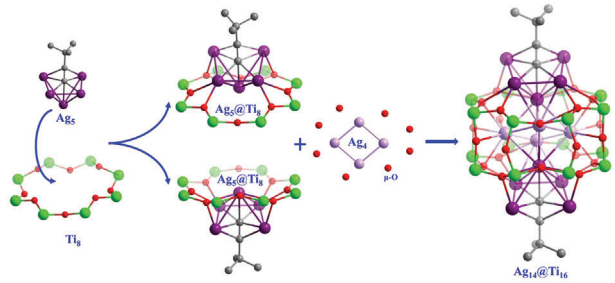

Figure 5. The possible formation mechanism of Ag14@Ti16 with atomically precise interfaces. Reprinted with permission.[19b] Copyright 2021 Wiley-VCH.

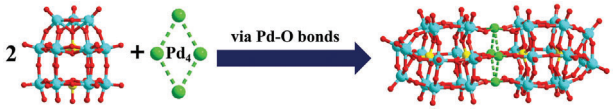

Figure 6. The schematic diagram of $Na_{16}[Pd_4(As_2W_{15}O_{56})_2]\cdot 65H_2O$ with atomically precise interfaces.

In this type of hybrid clusters, the ordered arrangement of adjacent POMs (or Ti-oxo clusters) and noble metal clusters gives an ideal model for metal-metal oxide interface. POMs as inorganic protecting agents could adjust the electron transfer, and provide an alternative for the construction of hybrid clusters with great stability. However, the vast majority of examples still have organic ligands on surface, hampering their practical applications. Using POMs as the sole protecting agents should be a promising way to address this issue.

2.3. Metal-Metal Oxide Interface in POM-Encapsulated Noble Metal Clusters

When using lacunary POMs as the sole protecting agents, the fully inorganic POM-encapsulated noble metal clusters can be obtained with noble metal cluster as cores and POM skeleton as shells.[20] In this section, we will focus on interface structures and the electron correlations between noble metals and POMs.

A sandwich-type hybrid cluster with the formula $Na_{16}[Pd_4(As_2W_{15}O_{56})_2]\cdot 65H_2O$ was synthesized by Kortz's group (**Figure 6**),[21] where four square-planar coordinated Pd^{2+} ions were coplanar with the rhombic configuration, and sandwiched by two Wells-Dawson $[\alpha\text{-}As_2W_{15}O_{56}]^{12-}$ units via seven oxygens.[21] The shift of anodic peaks to higher positive values in CV curves originated from the reduction of Pd^{2+} into Pd^0 due to its easy reduction ability. Based on the characteristics of the cluster, naturally, the cluster was employed as a catalyst for Suzuki–Miyaura reactions, exhibiting roughly equivalent performances compared with other Pd-based catalysts, because incorporated Pd^{2+} ions converted into Pd nanoparticles, confirmed by the photoelectron spectra of Pd $3d_{3/2}$ and $3d_{5/2}$ after catalysis again. $[\alpha\text{-}As_2W_{15}O_{56}]^{12-}$ units owned high negative charges and large sizes, and acted as stabilizing agents for Pd nanoparticles through sharing the negative charges, to improve the electronic properties and reactivity of Pd nanoparticles in solution.

The reaction between $Li_{17}(NH_4)_{21}[H_2P_8W_{48}O_{184}]$ ($\{P_8W_{48}\}$) and $[Pt(H_2O)_2(OH)_4]$ gave birth to $K_{22}(NH_4)_9H_3[\{Pt(OH)_3(H_2O)\}_6P_8W_{48}O_{184}]\cdot 79H_2O$ (1), in which $\{P_8W_{48}\}$ served as a multidentate ligand, locking $\{Pt(OH)_3(H_2O)\}$ between approximately two W–O units from two neighboring $\{P_2W_{12}\}$ moieties, forming a six Pt^{2+} center (**Figure 7a**).[22] Thus, its electrochemical behavior as well as $[Pt(H_2O)_2(OH)_4]$ was studied (Figure 7b). According to the CV plots, the conversion of Pt(IV) into Pt(II) was clearly observed in both cases, and the anodic peak of reoxidation was only found in 1. In $[Pt(H_2O)_2(OH)_4]$, there existed two cathodic peaks at 0.176 V and −0.375 V respectively, corresponding to the irreversible reduction of Pt(IV) into Pt(II) and Pt(II) to Pt(0) respectively, however, the relative anodic peak was missing. The comparison of their electrochemical behavior revealed $\{P_8W_{48}\}$ became the

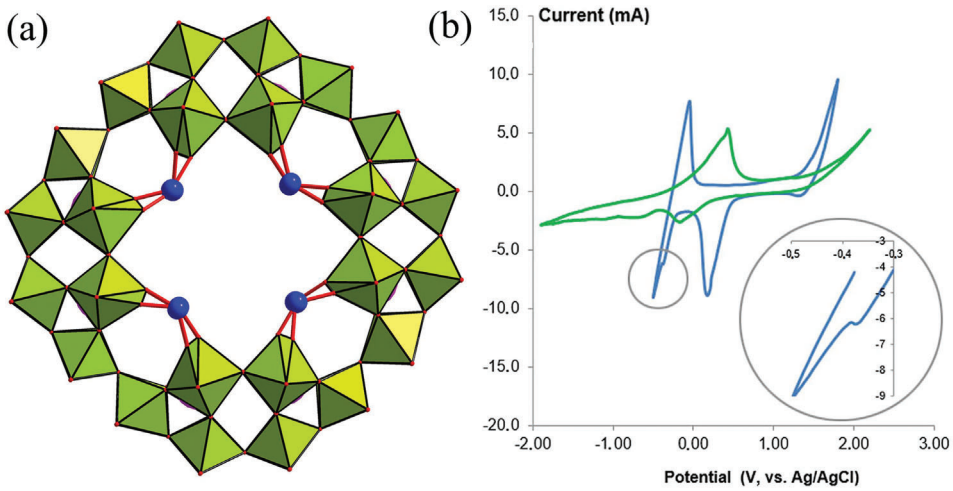

Figure 7. The structure of a) 1 and its electrochemical behavior as well as b) $[Pt(H_2O)_2(OH)_4]$. Reprinted with permission.[22] Copyright 2022 American Chemical Society.

electronic sponge, stored and transferred electrons, influencing redox behaviors of Pt(IV), promoting both reduction of Pt(IV) and reoxidation of Pt(II).

In this field, Suzuki and coworkers achieved several important breakthroughs. In 2019, they adopted a two-step assembly method to prepare $[Ag_{27}(Si_2W_{18}O_{66})_3]\cdot 12C_3H_4O_3\cdot 34H_2O$ (Ag27).[23a] The structural analysis revealed that Ag27 possessed an Ag_{27} nanocluster surrounded by three Dawson-type dimers $[Si_2W_{18}O_{66}]^{9-}$ ($\{Si_2W_{18}\}$) units through Ag-O-W coordination bonds. Additionally, Ag27 remained stable for at least seven days in solution under air atmosphere. DFT calculations were explored to calculate the molecular orbitals of Ag27 via the CAM-B3LYP functional. The highest occupied molecular orbitals (HOMO) mainly located in Ag_{27}^{17+} clusters, whose valence electrons were covered by POMs, making Ag27 extremely stable. Meanwhile, the lowest unoccupied molecular orbitals (LUMO) mainly originated from W d orbitals of $\{Si_2W_{18}\}$ units. Furthermore, time-dependent DFT calculations displayed that the absorption peak at ≈600 nm resulted from charge transfer inside Ag27. Another absorption peak at ≈530 nm was attributed to charge transfer from Ag_{27} clusters and O atoms to the POMs. It was the first case that the charge migrated from Ag clusters to POMs in the visible light area. Naturally, the cleavage reaction of dihydrogen (H_2) was first investigated using Ag27 as the catalyst.[23b] The synergistic effect between Ag_{27} and POMs was able to facilitate the efficient splitting of H_2 molecules, which converted into protons and electrons. H_2 cleavage process occurred at the interface formed by the Ag_{27} cluster and POMs. It was worth mentioning that, the original structure of Ag27 cluster still remained after H_2 cleavage reaction except that the valence state of Ag_{27} changed from +17 to +13 owing to the storage of electrons. Recently, they employed the large available space inside a ring-shaped $[P_8W_{48}O_{184}]^{40-}$ ($\{P_8W_{48}\}$) for the construction of silver clusters with exposed surfaces.[24] The reaction between $\{P_8W_{48}\}$ and excess AgOAc (OAc = acetate) generated Ag30 (**Figure 8a**). The investigation about redox property of Ag30 achieved an unexpected product Ag30' with $TBABH_4$ as the reducing agent at room temperature. The structure of Ag30' changed slightly, compared to Ag30, where four Ag atoms occupied two sites between $\{P_2W_{12}\}$ units, and the left Ag atoms divided into two hexagonal Ag_7 clusters and two triangular Ag_6 clusters. What's more, Ag30' could expose twelve Ag atoms at the window of the ring-shaped $\{P_8W_{48}\}$ skeleton. Notably, Ag30' exhibited an ultra-high stability in the atmosphere and the

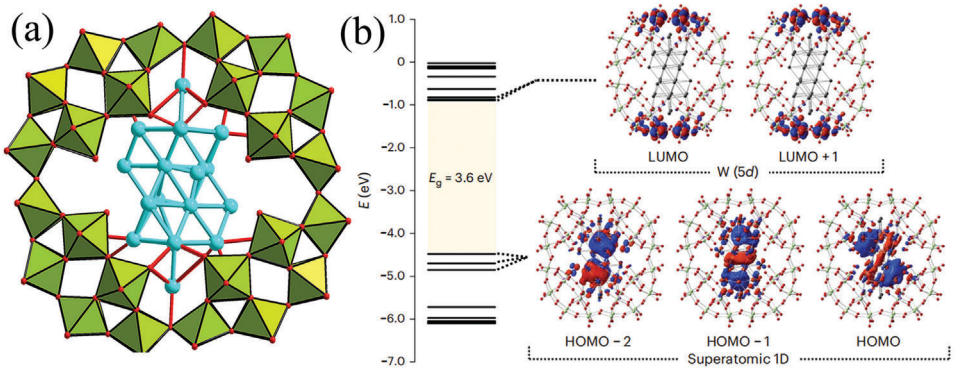

Figure 8. The structure of a) Ag30' and b) its molecular orbitals. Reprinted with permission.[24] Copyright 2023 Springer Nature.

solution. Partical HOMO were situated in silver clusters from Ag30, the other HOMO were left to POMs, revealed by DFT calculations. Meanwhile, all LUMO also delocalized over these silver clusters. While, in Ag30', all LUMO located at POMs, and the main HOMO lied in silver clusters (Figure 8b). This unique feature indicated that charge transfer could occur within silver clusters or between silver clusters and POMs. The UV–vis data of Ag30' owned some unique absorption bands at 420, 485, 550, and 650 nm respectively. The time-dependent DFT investigation was used to investigate the origin of these peaks. These characteristic peaks locating between 400 and 700 nm might belong to the electron migration inside Ag30'. The intense absorption peaks below 400 nm were ascribed to electrons migrations within silver clusters as well as charge transfer from silver clusters to POMs. Furthermore, Ag30' showed great catalytic performances for reducing nitrobenzene into aniline with H_2 under mild reaction conditions (4 atm H_2, 60 °C). Meanwhile, Ag30 displayed similar catalytic performances compared with Ag30', probably due to Ag30 could convert into Ag30' with the help of H_2.

In this year, the same group fabricated a novel anionic structure, $TBA_{16}H_8$-[$Au_8Ag_{26}(P_8W_{48}O_{184})$] (II) with a ring-shaped $\{P_8W_{48}\}$ holding a alloy Au-Ag nanocluster, in which a core–shell typed $\{Au_8Ag_{26}\}$ alloy nanocluster existed inside the cavity of ring-shaped $\{P_8W_{48}\}$ through the reaction between Ag30 and Au^+, and the oxidation states of P and W still maintained as +5 and +6 respectively.[25] In order to achieve a well-defined structure, a series of characterization methods, such as elemental analysis, Au L2-edge, and Ag K-edge X-ray absorption spectroscopy, had been carried out, and confirmed that there existed 8 Au atoms and 26 Ag atoms within per ring-shaped $\{P_8W_{48}\}$, indicating the successful generation of core–shell typed $\{Au_8Ag_{26}\}$ alloy nanocluster within ring-shaped $\{P_8W_{48}\}$, instead of the formation of bulk Au and large Au nanoparticles, and revealing the coordination numbers of Au and Ag were ≈6.6 and 3.5 respectively. The elemental analysis and acid–base titration revealed that the $\{Au_8Ag_{26}\}$ nanocluster achieved a charge of +16. X-ray photoelectron spectroscopy was employed to recognize its electronic states, where the spectra of Au 4f region confirmed the presence of Au^0, and the spectra of Ag 3d region exhibited that the molar ratio of Ag^+/Ag^0 was 16:10, consistent with the charges of $\{Au_8Ag_{26}\}$ alloy nanoclusters. DFT calculations clearly showed that some occupied orbitals with superatomic d-orbital-like feature distributed on the whole $\{Au_8Ag_{26}\}$ nanocluster, and unoccupied orbitals belonged to either the outer $\{P_8W_{48}\}$ or the inner Au-Ag nanoclusters. It should be mentioned that the UV–vis spectrum of II remained negligible changes for at least a week, implying that II was able to maintain its own structure and electronic state in the solution. Therefore, II was employed to evaluate its photocatalytic properties toward oxidation reactions in the existence of O_2, and showed to own superior photocatalytic aerobic oxidation of various substrates. After photocatalytic aerobic oxidation, the UV–vis spectra demonstrated that II held its structure and electronic state. Moreover, the Au L2-edge and Ag K-edge XANES spectra exhibited that the structure as well as the electronic state of $\{Au_8Ag_{26}\}$ nanocluster was well maintained, except the slightly changed arrangement of the surface Ag atoms.

Until now, metal-metal oxide interface in POM-encapsulated noble metal cluster focuses on the polytungstates, because polytungstates are a type of secure POMs, and still remain their configurations during the assembly process, beneficial for the formation of such clusters with stable and rigid skeletons. Varied valence states of polymolybdates, unique coordination patterns of polyvanadates and the instability of polyniobates are the obstacle for the development of hybrid clusters based on them. It is urgent to develop new approaches for preparing more architectures. Additionally, theoretical calculations prove that the surfaces or interfaces between noble metal clusters and POMs have a perceptible effect on not only their structures and electrical properties but also the catalytic pathway and the formation of products. Theoretical calculations also offer a powerful means to develop the structure-performance relationship from the atomic level. The described examples confirm that surfaces or interfaces are clearly present and charges transfer effectively from noble metal clusters to POMs.

It is still worth mentioning that, in some cases, lacunary POMs encapsulate noble metal clusters, which further template the formation of a shell of noble metal ions and organic ligands, forming a multilayer structure.[26] As their interface have been introduced in the Sections 2.1 and 2.3 separately, we will not discuss their structure in detail here.

Isolated inorganic hollow cages with fascinating architectures have attracted continuous attentions,[27] and win amusing applications in catalysis, proton conduction, etc.[28] Especially, inorganic hollow cages constructed from various POMs have some unique advantages: the size of obtained cages could be expanded due to nanosized POMs, the redox and catalytic activity could be well maintained in the final cages, available spaces allow the structure becoming designable platforms for unexpected applications. Continuous efforts have been contributed to the fabrication of POM-based cages, and an increasing number of achievements have been witnessed, for instance, the famous fullerene-like Mo_{132} cage.[29] Recently, our group has made some contributions, creating"Lantern" type Mo_{132} cage and the highest nuclearity Mo_{240} cage firstly.[30] Naturally, the reported POM-based cages could be used to prepare POM cage-encapsulated noble metal clusters with only noble metal-POM interfaces. Inorganic cages selected from the covered ones or the as-synthesized ones with new structures are employed as the matrix. Then, noble metal ions enter into the available space, and in situ turn into noble metal clusters within the cages using appropriate synthetic methods, generating POM cage-encapsulated noble metal clusters. Summarily, such hybrid clusters could be synthesized via the post-synthetic modification, making them become great candidates as molecular reactors.

3. Conclusion

POM-noble metal hybrid clusters are ideal models to understand the interfaces and interactions between noble metal clusters and POMs. The interactions and interfaces between them are proven to be the source of excellent catalytic performances. Understandings of interface structures at the atomic level can serve as the basic principles for catalyst design, yet is still a difficult task. These hybrid clusters are reasonable alternatives to address this issue due to their atomically precise structures and hybrid nature, based on which we could understand the interface structures and electronic correlations. However, most of them are trapped by organic ligands, hindering the exposure of noble metal clusters,

limiting their applications. POM-encapsulated noble metal clusters perfectly avoid the use of organic ligands, and are excellent alternatives.

In POM-templated noble metal clusters and POM-embedded noble metal clusters, the periphery of hybrid clusters are usually trapped by organic ligands, preventing the exposure of noble metal clusters, and act as appropriate shells to make the hybrid stable. In general, the selected ligands play a crucial role in tuning the electronic structures and potential applications of the resulting clusters, where the charge transfer often occurs between organic ligands and noble metal clusters, while POMs occasionally take participate in charge transfer. For example, some covered examples usually exhibit good photoluminescence promoted by the organic ligands, although good luminescent behaviors are unfavorable in the field of catalysis. It should be mentioned that there existed two kinds of interfaces: the outer organic interface of constructed from noble metal clusters and organic ligands and the inner inorganic interface of based on noble metal clusters and POMs. The reported achievements reveal that the inorganic interfaces based on noble metal clusters and POMs are responsive for the catalytic reaction. Based on this consideration, the family of POM-templated noble metal clusters cannot be employed in this field, because the inorganic interfaces exist inside the noble metal clusters template by POMs, and, in fact, there are no reports about such clusters in this field up to now. Therefore, if POM-embedded noble metal clusters are applied to the field of catalysis, it is necessary to remove organic ligands locating on the periphery of hybrid clusters in order to expose the inorganic interfaces. However, two large challenge need to be addressed: 1) how to remain the structure of clusters after removing organic ligands, 2) how about the stability during the catalysis without the protecting ligands.

For POMs-encapsulated noble metal clusters, POMs can adjust the structures of hybrid clusters, improve their stability and reactivity of noble metal clusters via balancing the charges of cationic noble metal clusters. The existence of POMs introduces new redox centers, and achieves charge transfer between noble metal clusters and POMs, further influencing the physical properties of the obtained clusters. Moreover, POMs can undergo structural isomerization or transformation induced by solvent etc., modifying the electronic interaction between noble metal clusters and POMs inside the generated hybrid clusters, and adjusting the catalytic performances of hybrid clusters. POMs, during the process of catalysis, not only provide a large available space for anchoring active sites, but also can optimize the electronic structures of hybrid clusters, benefitting the catalysis. It must be noted that only one kind of interface existed in such clusters: the inorganic interface resulting from noble metal clusters and POMs without no cover, meaning that no extra operations are required, and this kind of hybrid cluster could be directly explored in the field of catalysis. Until now, some great achievements have been uncovered, and it is noted that the surface-exposed inorganic interfaces formed by noble metal clusters and POMs are particularly related with the catalytic activity. So far, the development of this kind of clusters still remains in its infancy, and there is still a lot of room for development.

Compared to traditional metal clusters, POM-encapsulated noble metal clusters become beneficial to profoundly understand structure-property relationship and establish the mechanisms between surfaces and performances. Advanced characterization methods can provide clear experimental evidences for various applications. Furthermore, their precise structures provide great platforms for theoretical calculations, helping to reveal the mechanism together with the experimental evidences. Theoretical calculations to promote comprehensive understand interactions at the surface or interfaces, are of great importance in the rational design of their functional applications, accelerating the optimization of such hybrid clusters.

Several existing problems have to be considered, and are listed: 1) this kind of clusters is difficult to synthesize, because lacunary POMs must be employed. Additionally, used POMs are limited to polytungstate in these achievements, what about other lacunary POMs? 2) Their stability is a great obstacle for many applications, and needs to be verified in various environments. 3) The applications related to their physicochemical properties are barely developed. 4) Until now, almost only silver could combine with lacunary POMs, since POMs have a high affinity for silver. Other metals Pt, Pd and Au are very urgent to be explored for developing such hybrid clusters.

Consequently, the next attempts should be carried out in future to make further advances: 1) new synthetic methods, such as microwave or ionthermal approaches may be the reasonable choice in the presence of other lacunary POMs to build diversified and stable clusters. The combination of other lacunary POMs and new synthetic methods could be a suitable choice. 2) The stepwise synthesis method can be adopted to introduce other metals, preparing mixed metal cluster templated POMs. For instance, Ag is first introduced, and then other metals are used to expand metal clusters, developing mixed metal hybrid clusters. 3) The post-synthetic modification may be employed to prepare hybrid clusters only capped by lacunary POMs. Organic ligands can be used to prepare and stabilize metal clusters, then, lacunary POMs are employed to replace ligands, and obtain only lacunary POM modified metal clusters. 4) Precious silver clusters on metal oxides are explored in many catalytic reactions. We anticipate POM-encapsulated noble metal clusters with well-defined and exposed surfaces or interfaces will showcase exciting undiscovered properties owing to the acidity and redox property of POMs and the mix valence of noble metal clusters. Heterogeneous reactions closely related to their redox properties should be developed. Furthermore, the available space assembled by lacunary POMs not only accommodates noble metal clusters, but also owns free pores to allow the transfer of substrates. Later, we will concentrate on regulating inner noble metal clusters and outer POMs, achieving beautiful structures and excellent catalytic performances, and understanding catalytic reaction mechanisms to explore emerging heterogeneous reactions, even their industrial applications.

Acknowledgements

This work was financially supported by the NSFC (Grants 22225109, 22371080, 22071109, and 22301087), Shandong Provincial Natural Science Foundation (No. ZR2021MB005 and ZR2021MB074).

Conflict of Interest

The authors declare no conflict of interest.

Keywords

hybrid, interface, noble metal cluster, polyoxometalate, surface

Received: October 7, 2024
Revised: November 1, 2024
Published online:

[1] K. Liu, R. Qin, N. Zheng, *J. Am. Chem. Soc.* **2021**, *143*, 4483.
[2] a) S. Ji, Y. Chen, X. Wang, Z. Zhang, D. Wang, Y. Li, *Chem. Rev.* **2020**, *120*, 11900; b) K. Xia, K. Yamaguchi, K. Suzuki, *Angew. Chem., Int. Ed.* **2023**, *62*, 202214506.
[3] a) M. Cargnello, V. V. T. Doan-Nguyen, T. R. Gordon, R. E. Diaz, E. A. Stach, R. J. Gorte, P. Fornasiero, C. B. Murray, *Science* **2013**, *341*, 771; b) T. Akita, M. Kohyama, M. Haruta, *Acc. Chem. Res.* **2013**, *46*, 1773.
[4] L. Han, H. Cheng, W. Liu, H. Li, P. Ou, R. Lin, H.-T. Wang, C.-W. Pao, A. R. Head, C.-H. Wang, X. Tong, C.-J. Sun, W.-F. Pong, J. Luo, J.-C. Zheng, H. L. Xin, *Nat. Mater.* **2022**, *21*, 681.
[5] a) I. Fechete, Y. Wang, J. C. Védrine, *Catal. Today* **2012**, *189*, 2; b) J. Yan, B. K. Teo, N. Zheng, *Acc. Chem. Res.* **2018**, *51*, 3084.
[6] Y. Zhang, J. Liu, S.-L. Li, Z.-M. Su, Y.-Q. Lan, *Energy Chem* **2019**, *1*, 100021.
[7] a) C. Sun, B. K. Teo, C. Deng, J. Lin, G.-G. Luo, C.-H. Tung, D. Sun, *Coord. Chem. Rev.* **2021**, *427*, 213576; b) A. V. Virovets, E. Peresypkina, M. Scheer, *Chem. Rev.* **2021**, *121*, 14485.
[8] Y.-P. Xie, T. C. W. Mak, *Angew. Chem., Int. Ed.* **2012**, *51*, 8783.
[9] Z. Wang, R. K. Gupta, G.-G. Luo, D. Sun, *Chem. Rec.* **2020**, *20*, 389.
[10] a) J.-H. Huang, X.-Y. Dong, Y.-J. Wang, S.-Q. Zang, *Coord. Chem. Rev.* **2022**, *470*, 214729; b) Z.-J. Guan, J.-L. Zeng, Z.-A. Nan, X.-K. Wan, Y.-M. Lin, Q.-M. Wang, *Sci. Adv.* **2016**, *2*, 1600323; c) Q.-M. Wang, Y.-M. Lin, K.-G. Liu, *Acc. Chem. Res.* **2015**, *48*, 1570; d) O. Fuhr, S. Dehnen, D. Fenske, *Chem. Soc. Rev.* **2013**, *42*, 1871; e) R. Ge, X.-X. Li, S.-T. Zheng, *Coord. Chem. Rev.* **2021**, *435*, 213787.
[11] a) L.-M. Zhang, T. C. W. Mak, *J. Am. Chem. Soc.* **2016**, *138*, 2909; b) J.-Q. Wang, M.-H. Yan, S. Xiang, X. Fan, Z. Zhang, *Inorg. Chem. Front.* **2022**, *9*, 6330.
[12] B.-J. Yan, X.-S. Du, R.-W. Huang, J.-S. Yang, Z.-Y. Wang, S.-Q. Zang, T. C. W. Mak, *Inorg. Chem.* **2018**, *57*, 4828.
[13] G.-G. Gao, P.-S. Cheng, T. C. W. Mak, *J. Am. Chem. Soc.* **2009**, *131*, 18257.
[14] a) Z.-G. Jiang, K. Shi, Y.-M. Lin, Q.-M. Wang, *Chem. Commun.* **2014**, *50*, 2353; b) K.-G. Liu, X.-Y. Liu, Z.-J. Guan, K. Shi, Y.-M. Lin, Q.-M. Wang, *Chem. Commun.* **2016**, *52*, 3801; c) J.-Y. Wang, K.-G. Liu, Z.-J. Guan, Z.-A. Nan, Y.-M. Lin, Q.-M. Wang, *Inorg. Chem.* **2016**, *55*, 6833; d) J. Qiao, K. Shi, Q.-M. Wang, *Angew. Chem., Int. Ed.* **2010**, *49*, 1765.
[15] a) Z. Wang, H.-F. Su, C.-H. Tung, D. Sun, L.-S. Zheng, *Nat. Commun.* **2018**, *9*, 4407; b) S.-S. Zhang, H.-F. Su, Z. Wang, X.-P. W., W.-X. Chen, Q.-Q. Zhao, C.-H. Tung, D. Sun, L.-S. Zheng, *Chem. Eur. J.* **2018**, *24*, 1998.
[16] a) C. Zhan, J. M. Cameron, J. Gao, J. W. Purcell, D. L. Long, L. Cronin, *Angew. Chem., Int. Ed.* **2014**, *53*, 10362; b) Y. P. Xie, T. C. Mak, *J. Am. Chem. Soc.* **2011**, *133*, 3760;
[17] F. Gruber, M. Jansen, *Angew. Chem., Int. Ed.* **2010**, *49*, 4924.
[18] a) S. Chen, W.-H. Fang, L. Zhang, J. Zhang, *Angew. Chem., Int. Ed.* **2018**, *57*, 11252; b) X. Fan, F. Yuan, D. Li, S. Chen, Z. Cheng, Z. Zhang, S. Xiang, S.-Q. Zang, J. Zhang, L. Zhang, *Angew. Chem., Int. Ed.* **2021**, *60*, 12949; c) M.-Y. Gao, K. Wang, Y. Sun, D. Li, B.-Q. Song, Y. H. Andaloussi, M. J. Zaworotko, J. Zhang, L. Zhang, *J. Am. Chem. Soc.* **2020**, *142*, 12784.
[19] X.-M. Luo, C.-H. Gong, X.-Y. Dong, L. Zhang, S.-Q. Zang, *Nano Res.* **2021**, *14*, 2309.
[20] a) Y. Kikukawa, Y. Kuroda, K. Suzuki, M. Hibino, K. Yamaguchi, N. Mizuno, *Chem. Commun.* **2013**, *49*, 376; b) S. Sasaki, K. Yonesato, N. Mizuno, K. Yamaguchi, K. Suzuki, *Inorg. Chem.* **2019**, *58*, 7722; c) K. Yonesato, H. Ito, D. Yokogawa, K. Yamaguchi, K. Suzuki, *Angew. Chem., Int. Ed.* **2020**, *59*, 11778; d) N. V. Izarova, R. I. Maksimovskaya, S. Willbold, P. Kogerler, *Inorg. Chem.* **2014**, *53*, 11778.
[21] A. Rajan, A. S. Mougharbel, S. Bhattacharya, T. Nisar, V. Wagner, U. Kortz, *Inorg. Chem.* **2020**, *59*, 13042.
[22] A. A. Kuznetsova, V. V. Volchek, V. V. Yanshole, A. D. Fedorenko, N. B. Kompankov, V. V. Kokovkin, A. L. Gushchin, P. A. Abramov, M. N. Sokolov, *Inorg. Chem.* **2022**, *61*, 14560.
[23] a) K. Yonesato, H. Ito, H. Itakura, D. Yokogawa, T. Kikuchi, N. Mizuno, K. Yamaguchi, K. Suzuki, *J. Am. Chem. Soc.* **2019**, *141*, 19550; b) K. Yonesato, S. Yamazoe, D. Yokogawa, K. Yamaguchi, K. Suzuki, *Angew. Chem., Int. Ed.* **2021**, *60*, 16994.
[24] K. Yonesato, D. Yanai, S. Yamazoe, D. Yokogawa, T. Kikuchi, K. Yamaguchi, K. Suzuki, *Nat. Chem.* **2023**, *15*, 940.
[25] M. Kamachi, K. Yonesato, T. Okazaki, D. Yanai, S. Kikkawa, S. Yamazoe, R. Ishikawa, N. Shibata, Y. Ikuhara, K. Yamaguchi, K. Suzuki, *Angew. Chem., Int. Ed.* **2024**, *63*, 202408358.
[26] a) Z. Wang, H.-F. Su, M. Kurmoo, C.-H. Tung, D. Sun, L.-S. Zheng, *Nat. Commun.* **2018**, *9*, 2094; b) Y.-M. Su, Z. Wang, G.-L. Zhuang, Q.-Q. Zhao, X.-P. Wang, C.-H. Tung, D. Sun, *Chem. Sci.* **2019**, *10*, 564; c) J.-W. Liu, Z. Wang, Y.-M. Chai, M. Kurmoo, Q.-Q. Zhao, X.-P. Wang, C.-H. Tung, D. Sun, *Angew. Chem., Int. Ed.* **2019**, *58*, 6276; d) Z. Wang, Y.-J. Zhu, Y.-Z. Li, G.-L. Zhuang, K.-P. Song, Z.-Y. Gao, J.-M. Dou, M. Kurmoo, C.-H. Tung, D. Sun, *Nat. Commun.* **2022**, *13*, 1802.
[27] Q.-S. Lai, X.-X. Li, S.-T. Zheng, *Coord. Chem. Rev.* **2023**, *482*, 215077.
[28] J.-C. Liu, J.-W. Zhao, C. Streb, Y.-F. Song, *Coord. Chem. Rev.* **2022**, *471*, 214734.
[29] A. Müller, E. Krickemeyer, H. Bögge, M. Schmidtmann, F. Peters, *Angew. Chem., Int. Ed.* **1998**, *37*, 3359.
[30] a) J. Lin, N. Li, S. Yang, M. Jia, J. Liu, X.-M. Li, L. An, Q. Tian, L.-Z. Dong, Y.-Q. Lan, *J. Am. Chem. Soc.* **2020**, *142*, 13982; b) J. Liu, N. Jiang, J.-M. Lin, Z.-B. Mei, L.-Z. Dong, Y. Kuang, J.-J. Liu, S.-J. Yao, S.-L. Li, Y.-Q. Lan, *Angew. Chem. Int. Ed.* **2023**, *62*, 202304728.

Hai-Ning Wang received his BSc degree from Northeast Normal University in 2009, and in the same year, he joined Professor Zhong-Min Su to pursue his Ph.D. in physical chemistry from Northeast Normal University. In 2017, he carried out postdoctoral studies with Prof. Ya-Qian Lan in Inorganic Chemistry. Now, he is working at Shandong University of Technology. His research interests focus on the synthesis and properties of crystalline porous materials.

Xing Meng received her MSc in physical chemistry in 2012 from Northeast Normal University. In the same year, she joined Professor Hongjie Zhang to pursue her Ph.D. in inorganic chemistry at Changchun Institute of Applied Chemistry, Chinese Academy of Sciences. She is working at Shandong University of Technology. Her research interests focus on multi-functional porous materials and relevant properties.

Yitao Cao received his B.S. degree (2012) from Nanjing University. He obtained his Ph.D. degree (2017) from University of Chinese Academy of Science under the supervision of Prof. Tierui Zhang. He then joined Prof. Jianping Xie's group in National University of Singapore as a Postdoctoral Research Fellow from 2018 to 2023. In 2023, he joined Prof. Ya-Qian Lan's group at School of Chemistry, South China Normal University. He is now interested in the stoichiometric surface chemistry of inorganic clusters including POMs and metal clusters.

Shun-Li Li received her PhD (2008) from Northeast Normal University, under the supervision of Prof. Jian-Fang Ma. She then carried out postdoctoral studies in Environmental Chemistry with Prof. Zhong Min Su at NENU. In 2012, she joined Prof. Qiang Xu's group at National Institute of Advanced Industrial Science and Technology (Japan) as a JSPS invitation fellow. She is a professor of Chemistry at South China Normal University. Her current research interest lies in the syntheses, structures and properties of polyoxometalate-based materials.

Ya-Qian Lan received his PhD (2009) from Northeast Normal University, under the supervision of Prof. Zhong-Min Su. In 2010, he joined the National Institute of Advanced Industrial Science and Technology (Japan) working as a JSPS postdoctoral fellow. In 2012, he became a professor of chemistry at Nanjing Normal University. He joined South China Normal University in 2021, and is now a professor of chemistry. His current research interests focus on the synthesis of new crystalline materials and catalytic research related to clean energy applications.